

**INVESTIGATION OF MAGNESIUM DOPED CALCIUM COPPER
TITANATE ($\text{CaCu}_3\text{Ti}_4\text{O}_{12}$) ON Ca AND Cu SITE PREPARED BY SOLID
STATE REACTION METHOD**

MOHD FARIZ BIN AB RAHMAN

UNIVERSITI SAINS MALAYSIA

2013

**INVESTIGATION OF MAGNESIUM DOPED CALCIUM COPPER
TITANATE ($\text{CaCu}_3\text{Ti}_4\text{O}_{12}$) ON Ca AND Cu SITE PREPARED BY SOLID
STATE REACTION METHOD**

by

MOHD FARIZ BIN AB RAHMAN

**Thesis submitted in fulfillment of the requirements
for the degree of
Master of Science**

February 2013

ACKNOWLEDGEMENT

Bismillahirrahmanirrahim. With the name of Allah, The Most Beneficent and The Most Merciful. First and foremost, I would like to express my gratitude to Allah SWT for giving me strength and health in order to finish my studies in 2 years. On the other hand, my sincere appreciation also to the School of Materials and Mineral Resources Engineering (SMMRE), Universiti Sains Malaysia especially to the Dean of SMMRE, Professor Hanafi b. Ismail for provided good facilities to me during my studies here and to those who contributed to my work studies.

First, I want to acknowledge my high spirited supervisor, Associate Professor Dr. Sabar Derita Hutagalung for his major contributions to the successful of this project, as well as to my co-supervisor, Dr. Julie Juliewatty Mohamed for providing the knowledge based on the field of study.

I would also like to thank all the SMMRE's staffs, especially to Mr. Sharul Ami, Madam Fong, Mr. Razak, Mr. Kemuridan, Mr. Farid, Mr. Rashid, Mr. Khairi, Mr. Mokhtar, Mr. Zaini, Mr. Shahid and Mr. Syafiq for their technical support, as well as to my postgraduate friends; Azwadi, Wan Fahmin, Nik Akmar, Johari, Abdul Rashid, Zahirani, Mohamadariff, Norfadhilah, Shafiza and Sharifah Aisyah who always available for discussions.

Special thanks also to the Ministry of Higher Education, Malaysia for the financial support of MyBrain15 and to my family for their love and continued support.

TABLE OF CONTENTS

	Page
ACKNOWLEDGEMENT	ii
TABLE OF CONTENTS	iii
LIST OF TABLES	vii
LIST OF FIGURES	viii
LIST OF ABBREVIATIONS	xii
LIST OF MAIN SYMBOLS	xiv
ABSTRAK	xv
ABSTRACT	xvii
CHAPTER 1:INTRODUCTION	
1.1 Ceramics Materials	1
1.2 Problem Statement	3
1.3 Research Objective	6
1.4 Research Overview	6
CHAPTER 2:LITERATURE REVIEW	
2.1 Introduction	10
2.2 Dielectric Materials	11
2.3 Dielectric Properties	11
2.4 Polarization Effect	15
2.4.1 Frequency Dependence on the Dielectric Constant	17
2.5 Perovskite Structure	18

2.6	CaCu ₃ Ti ₄ O ₁₂	20
2.7	Grains Size Effect	23
	2.7.1 Internal Barrier Layer Capacitor	26
2.8	Processing Effect	28
2.9	Chemical Modifications on CaCu ₃ Ti ₄ O ₁₂	29
	2.9.1 Acceptor Dopant	30
	2.9.2 Donor Dopant	31
	2.9.3 Isovalent Substitution	32

CHAPTER 3: MATERIALS AND METHODOLOGY

3.1	Starting Materials	35
3.2	Processing Steps	35
	3.2.1 Composition Formulation	35
	3.2.2 Mixing Process	37
	3.2.3 Calcination	38
	3.2.4 De-agglomeration	40
	3.2.5 Uniaxial Pressing	41
	3.2.6 Sintering	41
3.3	Characterization Techniques	43
	3.3.1 Phase Structure Analysis	43
	3.3.2 Microstructures and Elemental Composition Analysis	44
	3.3.3 Density and Porosity Test	45
	3.3.4 Dielectric Properties Measurement	46

CHAPTER 4: RESULTS AND DISCUSSION

4.1	Properties of Starting Materials	48
4.1.1	Calcium Carbonate (CaCO_3) Powder	48
4.1.2	Copper Oxide (CuO) Powder	50
4.1.3	Titanium Oxide (TiO_2) Powder	51
4.1.4	Magnesium Oxide (MgO) Powder	53
4.2	Undoped $\text{CaCu}_3\text{Ti}_4\text{O}_{12}$ (CCTO)	54
4.2.1	Phase Structure of $\text{CaCu}_3\text{Ti}_4\text{O}_{12}$	56
4.2.2	Microstructure Analysis of $\text{CaCu}_3\text{Ti}_4\text{O}_{12}$	59
4.2.3	Density and Porosity of $\text{CaCu}_3\text{Ti}_4\text{O}_{12}$	60
4.3	Mg-doped CCTO on Cu site ($\text{CaCu}_{3-x}\text{Mg}_x\text{Ti}_4\text{O}_{12}$)	61
4.3.1	Phase Structure of $\text{CaCu}_{3-x}\text{Mg}_x\text{Ti}_4\text{O}_{12}$	62
4.3.2	Microstructure of Sintered $\text{CaCu}_{3-x}\text{Mg}_x\text{Ti}_4\text{O}_{12}$	66
4.3.3	Density and Porosity of $\text{CaCu}_{3-x}\text{Mg}_x\text{Ti}_4\text{O}_{12}$	71
4.3.4	Dielectric Behavior of $\text{CaCu}_{3-x}\text{Mg}_x\text{Ti}_4\text{O}_{12}$	72
4.4	Mg-doped CCTO on Ca site ($\text{Ca}_{1-x}\text{Mg}_x\text{Cu}_3\text{Ti}_4\text{O}_{12}$)	77
4.4.1	Phase Structure of $\text{Ca}_{1-x}\text{Mg}_x\text{Cu}_3\text{Ti}_4\text{O}_{12}$	78
4.4.2	Microstructure of Sintered $\text{Ca}_{1-x}\text{Mg}_x\text{Cu}_3\text{Ti}_4\text{O}_{12}$	81
4.4.3	Density and Porosity of $\text{Ca}_{1-x}\text{Mg}_x\text{Cu}_3\text{Ti}_4\text{O}_{12}$	84
4.4.4	Dielectric Behavior of $\text{Ca}_{1-x}\text{Mg}_x\text{Cu}_3\text{Ti}_4\text{O}_{12}$	85
4.5	Dielectric Properties Comparison Between $\text{CaCu}_{3-x}\text{Mg}_x\text{Ti}_4\text{O}_{12}$ and $\text{Ca}_{1-x}\text{Mg}_x\text{Cu}_3\text{Ti}_4\text{O}_{12}$ Samples	90

CHAPTER 5: CONCLUSION AND RECOMMENDATION

5.1 Conclusion 94

5.2 Recommendation for Future Research 95

REFERENCES 96

APPENDIX 101

LIST OF PUBLICATION AND CONFERENCES 107

LIST OF TABLES

Table 1.1	Summaries of scope of work from the previous studies and the recent study.	5
Table 2.1	The value of dielectric constant of materials at measured at 1 MHz	15
Table 2.2	Dielectric properties data and lattice parameter data for $\text{ACu}_3\text{Ti}_4\text{O}_{12}$ phases at 25°C	22
Table 3.1	Details of starting materials	35
Table 3.2	Quantity of starting materials to prepare $\text{CaCu}_{3-x}\text{Mg}_x\text{Ti}_4\text{O}_{12}$	36
Table 3.3	Quantity of starting materials to prepare $\text{Ca}_{1-x}\text{Mg}_x\text{Cu}_3\text{Ti}_4\text{O}_{12}$	37
Table 3.4	Sample codes for Mg-doped CCTO	37
Table 4.1	Relative density and porosity of CCTO samples sintered at different temperatures	61
Table 4.2	Lattice parameter and crystallite size measurement of $\text{CaCu}_{3-x}\text{Mg}_x\text{Ti}_4\text{O}_{12}$ samples with various compositions of MgO	65
Table 4.3	Average grain size of $\text{CaCu}_{3-x}\text{Mg}_x\text{Ti}_4\text{O}_{12}$ samples with various compositions of MgO	67
Table 4.4	Lattice parameter and crystallite size measurement of $\text{Ca}_{1-x}\text{Mg}_x\text{Cu}_3\text{Ti}_4\text{O}_{12}$ samples with various compositions of MgO	81
Table 4.5	Average grain size of $\text{Ca}_{1-x}\text{Mg}_x\text{Cu}_3\text{Ti}_4\text{O}_{12}$ samples with various compositions of MgO	83

LIST OF FIGURES

Figure 1.1	Process flow of undoped and Mg-doped CCTO with $x = 0.00, 0.01, 0.02, 0.03, 0.05, 0.10$	9
Figure 2.1	A parallel-plate capacitor (a) when a vacuum is present and (b) when a dielectric material is present	14
Figure 2.2	Schematic representation of different mechanism of polarization (a) Electronic polarization (b) Ionic polarization (c) Orientation polarization	17
Figure 2.3	Variation of dielectric constant with the frequency of an alternating dielectric field	18
Figure 2.4	Unit cell of perovskite cubic structures	19
Figure 2.5	Unit cell of body-centered cubic $\text{CaCu}_3\text{Ti}_4\text{O}_{12}$ in the $\text{Im}\bar{3}$ space group	21
Figure 2.6	SEM images of CCTO surface of sintered pellets No. 1 and No. 5 at 1000°C for 20 hours	24
Figure 2.7	Dielectric constant of different samples using same sintering profile	25
Figure 2.8	Internal barrier layer capacitance (IBLC) model structure in CCTO	27
Figure 2.9	Equivalence circuit of parallel capacitor and resistor	28
Figure 3.1	Temperature profile for calcination process of undoped $\text{CaCu}_3\text{Ti}_4\text{O}_{12}$ and Mg-doped $\text{CaCu}_3\text{Ti}_4\text{O}_{12}$ powder	40
Figure 3.2	Temperature profile for sintering process of undoped $\text{CaCu}_3\text{Ti}_4\text{O}_{12}$ and Mg-doped $\text{CaCu}_3\text{Ti}_4\text{O}_{12}$ pellet	43
Figure 3.3	Schematic diagram of dielectric measurement using Impedance	47

	Analyzer	
Figure 4.1	SEM micrograph of CaCO ₃ powders	49
Figure 4.2	XRD pattern of CaCO ₃ powders	49
Figure 4.3	SEM micrograph of CuO powders	50
Figure 4.4	XRD pattern of CuO powders	51
Figure 4.5	SEM micrograph of TiO ₂ powders	52
Figure 4.6	XRD pattern of TiO ₂ powders	52
Figure 4.7	SEM micrograph of MgO powders	53
Figure 4.8	XRD pattern of MgO powders	54
Figure 4.9	Mixed powder of CCTO after milling process	55
Figure 4.10	Yellowish powder of CCTO after calcination process	55
Figure 4.11	(a) Calcined green body after compaction and (b) sintered CCTO pellets	56
Figure 4.12	XRD pattern of CCTO powders mixed using (a) deionized water (b) acetone (c) ethanol were calcined at 900°C for 12 hours	57
Figure 4.13	XRD pattern of CCTO sample sintered for 10 hours at (a) 1020°C (b) 1030°C and (c) 1040°C	58
Figure 4.14	SEM micrograph of CCTO samples sintered at (a) 1020°C (b) 1030°C and (c) 1040°C for 10 hours	60
Figure 4.15	XRD pattern of CaCu _{3-x} Mg _x Ti ₄ O ₁₂ powders with different Mg doping concentrations calcined at 900°C for 12 hours	62
Figure 4.16	XRD pattern of CaCu _{3-x} Mg _x Ti ₄ O ₁₂ samples with different Mg doping concentrations sintered at 1030°C for 10 hours	63
Figure 4.17	Close-up of XRD patterns of CaCu _{3-x} Mg _x Ti ₄ O ₁₂ samples with different Mg doping concentrations	65

Figure 4.18	SEM micrographs of $\text{CaCu}_{3-x}\text{Mg}_x\text{Ti}_4\text{O}_{12}$ samples with different Mg doping concentrations sintered at 1030°C for 10 hours	67
Figure 4.19	EDX analysis result of Mg-doped CCTO sample spotted at grain and grain boundary layer	69
Figure 4.20	Fracture surface of sintered $\text{CaCu}_{3-x}\text{Mg}_x\text{Ti}_4\text{O}_{12}$ samples with Mg doping concentration (a) $x = 0.00$, (b) $x = 0.01$ and (c) $x = 0.10$	70
Figure 4.21	Relative density and porosity of $\text{CaCu}_{3-x}\text{Mg}_x\text{Ti}_4\text{O}_{12}$ samples with different Mg doping concentrations	72
Figure 4.22	Frequency dependence of dielectric constant of $\text{CaCu}_{3-x}\text{Mg}_x\text{Ti}_4\text{O}_{12}$ samples as a function of Mg doping concentrations	74
Figure 4.23	Dielectric constant of $\text{CaCu}_{3-x}\text{Mg}_x\text{Ti}_4\text{O}_{12}$ samples with different Mg doping concentrations at various frequencies (a) 1 MHz, 10 MHz, 100 MHz and 1 GHz, and (b) close up of dielectric constant at 100 MHz and 1 GHz	75
Figure 4.24	Frequency dependence of dielectric loss of $\text{CaCu}_{3-x}\text{Mg}_x\text{Ti}_4\text{O}_{12}$ samples as a function of Mg doping concentrations	77
Figure 4.25	XRD pattern of $\text{Ca}_{1-x}\text{Mg}_x\text{Cu}_3\text{Ti}_4\text{O}_{12}$ powders with different Mg doping concentrations calcined at 900°C for 12 hours	78
Figure 4.26	XRD pattern of $\text{Ca}_{1-x}\text{Mg}_x\text{Cu}_3\text{Ti}_4\text{O}_{12}$ samples with different Mg doping concentrations sintered at 1030°C for 10 hours	79
Figure 4.27	Close-up of XRD patterns of $\text{Ca}_{1-x}\text{Mg}_x\text{Cu}_3\text{Ti}_4\text{O}_{12}$ samples with different Mg doping concentrations	80
Figure 4.28	SEM micrographs of sintered $\text{Ca}_{1-x}\text{Mg}_x\text{Cu}_3\text{Ti}_4\text{O}_{12}$ samples with different Mg doping concentrations sintered 1030°C for 10 hours	83
Figure 4.29	Fracture surface of sintered $\text{Ca}_{1-x}\text{Mg}_x\text{Cu}_3\text{Ti}_4\text{O}_{12}$ samples with Mg	84

doping concentration (a) $x = 0.01$, (b) $x = 0.02$ and (c) 0.10

- Figure 4.30 Relative density and porosity of $\text{Ca}_{1-x}\text{Mg}_x\text{Cu}_3\text{Ti}_4\text{O}_{12}$ samples with 85
different Mg doping concentrations
- Figure 4.31 Frequency dependence of dielectric constant of Ca_{1-x} 86
 $\text{Mg}_x\text{Cu}_3\text{Ti}_4\text{O}_{12}$ samples as a function of Mg doping concentrations
- Figure 4.32 Dielectric constant of $\text{Ca}_{1-x}\text{Mg}_x\text{Cu}_3\text{Ti}_4\text{O}_{12}$ samples with different 88
Mg doping concentrations at various frequencies (a) 1 MHz, 10
MHz, 100 MHz and 1 GHz, and (b) close up of dielectric constant
at 100 MHz and 1 GHz
- Figure 4.33 Frequency dependence of dielectric loss of $\text{Ca}_{1-x}\text{Mg}_x\text{Cu}_3\text{Ti}_4\text{O}_{12}$ 90
samples as a function of Mg doping concentrations
- Figure 4.34 Dielectric constant of $\text{CaCu}_{3-x}\text{Mg}_x\text{Ti}_4\text{O}_{12}$ and $\text{Ca}_{1-x}\text{Mg}_x\text{Cu}_3\text{Ti}_4\text{O}_{12}$ 91
samples versus Mg doping concentrations measured at different
frequencies (a) 1 MHz (b) 1 GHz
- Figure 4.35 Dielectric loss of $\text{CaCu}_{3-x}\text{Mg}_x\text{Ti}_4\text{O}_{12}$ and $\text{Ca}_{1-x}\text{Mg}_x\text{Cu}_3\text{Ti}_4\text{O}_{12}$ 93
samples versus Mg doping concentrations measured at different
frequencies (a) 1 MHz (b) 1 GHz

LIST OF ABBREVIATIONS

- $\text{CaCu}_3\text{Ti}_4\text{O}_{12}$: Calcium copper titanate
- $\text{CaCu}_{2.99}\text{Mg}_{0.01}\text{Ti}_4\text{O}_{12}$: Calcium copper titanate with 0.01 mole fraction or 1 mol% of magnesium doped at Cu site
- $\text{CaCu}_{2.98}\text{Mg}_{0.02}\text{Ti}_4\text{O}_{12}$: Calcium copper titanate with 0.02 mole fraction or 2 mol% of magnesium doped at Cu site
- $\text{CaCu}_{2.97}\text{Mg}_{0.03}\text{Ti}_4\text{O}_{12}$: Calcium copper titanate with 0.03 mole fraction or 3 mol% of magnesium doped at Cu site
- $\text{CaCu}_{2.95}\text{Mg}_{0.05}\text{Ti}_4\text{O}_{12}$: Calcium copper titanate with 0.05 mole fraction or 5 mol% of magnesium doped at Cu site
- $\text{CaCu}_{2.90}\text{Mg}_{0.10}\text{Ti}_4\text{O}_{12}$: Calcium copper titanate with 0.10 mole fraction or 10 mol% of magnesium doped at Cu site
- $\text{Ca}_{0.99}\text{Mg}_{0.01}\text{Cu}_3\text{Ti}_4\text{O}_{12}$: Calcium copper titanate with 0.01 mole fraction or 1 mol% of magnesium doped at Ca site
- $\text{Ca}_{0.98}\text{Mg}_{0.02}\text{Cu}_3\text{Ti}_4\text{O}_{12}$: Calcium copper titanate with 0.02 mole fraction or 2 mol% of magnesium doped at Ca site
- $\text{Ca}_{0.97}\text{Mg}_{0.03}\text{Cu}_3\text{Ti}_4\text{O}_{12}$: Calcium copper titanate with 0.03 mole

- fraction or 3 mol% of magnesium doped
at Ca site
- $\text{Ca}_{0.95}\text{Mg}_{0.05}\text{Cu}_3\text{Ti}_4\text{O}_{12}$: Calcium copper titanate with 0.05 mole
fraction or 5 mol% of magnesium doped
at Ca site
- $\text{Ca}_{0.90}\text{Mg}_{0.10}\text{Cu}_3\text{Ti}_4\text{O}_{12}$: Calcium copper titanate with 0.10 mole
fraction or 10 mol% of magnesium
doped at Ca site
- SEM : Scanning Electron Microscopy
- XRD : X-ray Diffraction
- EDX : Energy Dispersive X-ray

LIST OF MAIN SYMBOLS

%	Percentage
°	Degree
°C	Degree Celsius
°C/min	Degree Celsius per minutes
MPa	Megapascal
g	Gram
nm	Nanometer
μm	Micrometer
mm	Milimeter
g/cm ³	Gram per cubic centimeter
wt %	Weight percent
λ	Wave length
s	Second
min	Minutes
ε	Permittivity
tan δ	Tangent loss
MHz	Megahertz
GHZ	Gigahertz

**KAJIAN KE ATAS CALCIUM COPPER TITANATE ($\text{CaCu}_3\text{Ti}_4\text{O}_{12}$) DIDOP
MAGNESIUM PADA KEDUDUKAN Ca DAN Cu DISEDIAKAN MELALUI
KAEDAH TINDAK BALAS PEPEJAL**

ABSTRAK

Penyelidikan ini mengkaji kesan pendopan magnesium (Mg) ke atas sifat-sifat dielectrik $\text{CaCu}_3\text{Ti}_4\text{O}_{12}$ (CCTO). CCTO tulen dan CCTO yang didop Mg pada kedudukan Ca dan Cu ($\text{Ca}_{1-x}\text{Mg}_x\text{Cu}_3\text{Ti}_4\text{O}_{12}$, $\text{CaCu}_{3-x}\text{Mg}_x\text{Ti}_4\text{O}_{12}$ dan $\text{Ca}_{1-x}\text{Mg}_x\text{Cu}_3\text{Ti}_4\text{O}_{12}$) telah disediakan melalui kaedah tindak balas keadaan pepejal. Bahan mentah CaCO_3 , CuO , TiO_2 dan MgO telah dikisar basah menggunakan tiga agen pembasahan iaitu aseton, air ternyah ion dan etanol. Analisis XRD pada serbuk kalsin menunjukkan pembentukan fasa $\text{CaCu}_3\text{Ti}_4\text{O}_{12}$ (CCTO) dengan kehadiran sedikit fasa kedua (CuO dan TiO_2). Proses pencampuran menggunakan air ternyah ion memberikan campuran yang lebih baik dan menghasilkan fasa CCTO dengan keamatan yang lebih tinggi selepas dikalsin pada suhu 900°C selama 12 jam. Pelet yang ditekan telah disinter pada suhu 1020°C , 1030°C dan 1040°C selama 10 jam. Profil pensinteran pada $1030^\circ\text{C}/10$ jam telah dikenalpasti sebagai parameter yang optimum dalam pembentukan fasa tunggal CCTO dengan pertumbuhan butiran yang kecil, ketumpatan yang tinggi dan keliangan yang rendah. Komposisi MgO dipelbagai dari 1 hingga 10 peratus mol untuk kedudukan Ca dan Cu dalam struktur CCTO. Imej SEM menunjukkan saiz butiran semakin meningkat dengan peningkatan kepekatan bahan dop. Ketumpatan dan keliangan sampel yang disinter telah ditambah baik dengan pendopan. Sampel $\text{CaCu}_{3-x}\text{Mg}_x\text{Ti}_4\text{O}_{12}$ dengan $x = 0.01$ menunjukkan pemalar dielektrik yang paling tinggi iaitu 1821 pada frekuensi 1 MHz

dan 85 pada 1 GHz. Disamping itu, sampel $\text{Ca}_{1-x}\text{Mg}_x\text{Cu}_3\text{Ti}_4\text{O}_{12}$ dengan $x = 0.05$ menunjukkan pemalar dielektrik yang paling tinggi iaitu 1278 pada 1 MHz. Sementara itu, ujikaji menunjukkan penurunan ketara dalam lesapan dielektrik pada sampel didop dengan Mg. Lesapan dielektrik menurun daripada 0.053 ke 0.007 untuk sampel yang didop pada kedudukan Ca pada 1 GHz, manakala sampel yang didop pada kedudukan Cu tidak menunjukkan penambahbaikan yang ketara. Oleh itu, pendopan Mg boleh digunakan untuk menambah baik sifat dielektrik bagi CCTO.

**INVESTIGATION OF MAGNESIUM DOPED CALCIUM COPPER
TITANATE ($\text{CaCu}_3\text{Ti}_4\text{O}_{12}$) ON Ca AND Cu SITE PREPARED BY SOLID
STATE REACTION METHOD**

ABSTRACT

In this research, the effect of magnesium (Mg) dopant on dielectric properties of $\text{CaCu}_3\text{Ti}_4\text{O}_{12}$ (CCTO) was investigated. Undoped CCTO and Mg-doped CCTO on Ca and Cu site ($\text{Ca}_{1-x}\text{Mg}_x\text{Cu}_3\text{Ti}_4\text{O}_{12}$ and $\text{CaCu}_{3-x}\text{Mg}_x\text{Ti}_4\text{O}_{12}$ have been prepared by solid state reaction method. Starting materials of CaCO_3 , CuO , TiO_2 and MgO were wet milled for 1 hour by using three wetting agents which are acetone, deionized water and ethanol. XRD analysis on calcined powders shows the formation of $\text{CaCu}_3\text{Ti}_4\text{O}_{12}$ (CCTO) phase with present of minor secondary phases (CuO and TiO_2). Mixing process in deionized water gave better mixing and produces higher intensity of CCTO phase after calcined at 900°C for 12 hours. Compacted pellet was sintered at 1020°C , 1030°C and 1040°C for 10 hours. The sintering profile of $1030^\circ\text{C}/10$ hours was identified as an optimum parameter in the formation of single phase of CCTO with fine grain growth, high density and low porosity. MgO composition had been verified from 1 until 10 mole percent for Ca and Cu site of CCTO structure. SEM images show that the grain size becomes larger with increasing the concentration of dopant. Density and porosity of sintered samples were improved by dopant. The $\text{CaCu}_{3-x}\text{Mg}_x\text{Ti}_4\text{O}_{12}$ samples with $x = 0.01$ exhibited the highest dielectric constant of 1821 at frequency 1 MHz and 85 at 1 GHz. Besides, the $\text{Ca}_{1-x}\text{Mg}_x\text{Cu}_3\text{Ti}_4\text{O}_{12}$ samples with $x = 0.05$ exhibited highest dielectric constant of 1278 at 1 MHz. Meanwhile, the results show a significant decrement in dielectric loss for the

Mg-doped samples. The dielectric loss was decreased from 0.053 to 0.007 for the sample doped at Ca site at 1 GHz, while for Cu site, no significant improvement. Therefore, Mg dopant can be used to improve the dielectric behavior of CCTO.

CHAPTER 1

INTRODUCTION

1.1 Electroceramic

Ceramics are classified as an inorganic materials and it is consisting of metallic and nonmetallic elements. Inorganic materials are compounds that most typically oxides, carbides, and nitrides. The ‘ceramic’ phrase comes from Greek word, *keramikos* which is stand for “burnt stuff”. It shows that a firing process or high temperature heat treatment is required in order to get the desirable properties of the ceramic materials (Callister, 2007). The common properties of ceramic materials are hard, brittle, high compression strength and low shearing strength. Besides, it is also able to withstand at high temperatures and harsh environment compared to the metal and polymers. Ceramic materials are mostly act as insulator because it cannot conduct heat and electricity.

The development of traditional ceramics to advanced ceramics has begun and expanded especially in our advanced technologies nowadays. Particularly, the electrical, optical, and magnetic properties of ceramic materials have been explored in order to develop a new product. Beginning year 1910 onwards, many ceramics materials have been synthesized for the development of electronic materials. The substances such as manganese zinc ferrites and nickel-zinc were used as choke and transformer core materials. The products were used for high frequencies application (beyond 1 MHz) due to high resistivity and low susceptibility to eddy currents (Moulson and Herbert, 2003).

Electroceramic is referring as ceramics materials that have been created for electrical, optical and magnetic properties. The electrical properties that were usually

stressed are capacitance, conductivity, resistivity, dielectric constant and dielectric loss. The electroceramic materials can be used for the applications as capacitor, filter, resonator, sensor, actuator, etc. Capacitor is one of the main device which are very important in electronic circuit because it can be use as AC-DC separation, coupling and decoupling, filtering, power factor correction and energy storage (Kao, 2004). The size of electronic devices can also be decrease since high dielectric constant allows smaller capacitive components to be made. The attempt to raise dielectric constant and minimize dielectric loss will increase the effectiveness of dielectric materials (Hutagalung et al., 2009).

Dielectric materials are an electrical insulator but it can support the electric field effectively. Most of dielectric materials are solid but some liquids and gases such as distilled water and dry air can also be used as dielectric materials (Rouse, 2010). The important property of dielectric material is that it can sustain the electric field with minimal dissipation of energy which in the form of heat (Kao, 2004). In practice, all dielectric exhibit some conductivity, generally proportional with temperature and applied field (McGraw-Hill, 2002). If the applied voltage across dielectric material is too large or applied field becomes too intense, the material will start to conduct current. This incident is called dielectric breakdown (Callister, 2007).

Calcium copper titanate, $\text{CaCu}_3\text{Ti}_4\text{O}_{12}$ (CCTO) is known as one of the electroceramic materials. Subramanian et al. (2000) reported that CCTO exhibited high dielectric constant which is about $\sim 10^4$ and Ramirez et al. (2000) stated that CCTO also has good temperature stability in a wide temperature range 100 to 400 K. CCTO is different from other perovskite material that has ferroelectric properties such as BaTiO_3 . Near its Curie point, BaTiO_3 shows a great enhancement in dielectric constant but it can also have unfavorable structural phase transition due to

strong temperature dependence. Meanwhile, the permittivity of CCTO is stable at high value from 100 to 400 K. The dielectric constant of CCTO was found drops rapidly to a value around 100 when the temperature was below 100 K but it is not accompanied by any structural phase transition.

1.2 Problem Statement

As reported by Subramanian et al. (2000), $\text{CaCu}_3\text{Ti}_4\text{O}_{12}$ (CCTO) exhibited very high dielectric constant which can reach up to 10^4 at 1 kHz. Unfortunately, it still cannot be commercialize for practical applications due to its high dielectric loss. Guillemet-Fritsch et al. (2006) reported that the average value of dielectric loss of CCTO at room temperature is 0.5 at 1 kHz. This value is considered high for commercial device application. Therefore, the dielectric loss of CCTO has to be improved in order enhance the performance of CCTO based devices.

The origin high dielectric loss of CCTO is still being discussed among researchers. There are many factors which cause dielectric loss in this complex ceramic compound such as the contributions of an extrinsic nature which associated with imperfections in the crystal structure such as microstructural defects, microcracks, grain boundary, porosity and impurities (Alford and Penn, 1996). High grain boundary resistance will decrease the dielectric loss (Makcharoen, 2012). Meanwhile, Moulson and Herbert (2003) stated that even though small amount of secondary phases may present, it can give effect on the properties of the material by the way in which they are distributed.

Several methods have been studied by researchers and they had proposed many ways to reduce the dielectric loss of CCTO. The most popular techniques is by doping CCTO with other elements such as Nb-doped CCTO (Sulaiman et al., 2010),

Pb-doped CCTO (Bender & Pan, 2009), Zn-doped CCTO (Hutagalung et al., 2009) and Sr-doped CCTO (Mu et al., 2009). Dopants are added in order to improve densification, enhance material transport rate and increase lattice diffusivity of the particles during sintering process. Improving densification can reduce porosities in the CCTO sample, hence contribute to reduce the dielectric loss. Besides, the dopant attracts and neutralizes jumping electrons between the CCTO ions which leads to the dielectric loss reduced (Sharif, 2010).

Several researchers had also studied the effect of magnesium oxide (MgO) on dielectric properties of CCTO. They claimed that with the addition of Mg as a dopant, the dielectric properties of CCTO especially dielectric loss can be improved. Li et al. (2010) concluded that $\text{Ca}_{1-x}\text{Mg}_x\text{Cu}_3\text{Ti}_4\text{O}_{12}$ with $x = 0.05$ had dielectric loss around 0.04 at 1 kHz. It was better compared with the undoped CCTO sample that can only exhibit 0.39 at 1 kHz. Meanwhile, Li et al. (2008) reported that dielectric loss for $\text{CaCu}_{3-x}\text{Mg}_x\text{Ti}_4\text{O}_{12}$ at 200 kHz when $x = 0.3$ can be reduce to ~ 0.052 . Furthermore, the dielectric loss data show that the Mg-doped CCTO samples exhibited lower dielectric lost than the undoped CCTO sample in the frequency range from 200 Hz to 200 kHz. So, it shows that Mg dopant can be used to reduce the dielectric loss of CCTO even though the dopant was used to substitute parental atom at different site of CCTO structure (Ca and Cu site).

However, there are no reports about the dielectric behavior of CCTO at higher frequencies (1 MHz to 1 GHz). Nowadays, there are many devices that operate at high frequency such as wireless communication devices. As CCTO have potential for high frequency devices application, the knowledge of high frequency properties of CCTO is also necessary. Therefore, this study was focused on the investigation of magnesium doped CCTO at Ca and Cu site of CCTO and the

dielectric properties of the samples were measured at high frequency range from 1 MHz to 1 GHz.

Table 1.1: Summaries of scope of work from the previous studies and the current study.

Titles	Scope of work
<p>Enhanced dielectric responses in Mg-doped $\text{CaCu}_3\text{Ti}_4\text{O}_{12}$ (Li et al., 2008).</p>	<p>-Doped by MgO on Cu site of CCTO with 10 to 50 mol% of doping.</p> <p>-Dry milling process.</p> <p>-The dielectric properties of CCTO were measured at frequencies range from 200 Hz to 200 kHz.</p>
<p>Enhanced Dielectric Response in Mg-doped $\text{CaCu}_3\text{Ti}_4\text{O}_{12}$ Ceramics (Li et al., 2010).</p>	<p>-Doped by MgO on Ca site of CCTO with 1 to 10 mol% of doping.</p> <p>-Dry milling process.</p> <p>-The dielectric properties of CCTO were measured at frequencies range from 20 Hz to 1 MHz.</p>
<p>Dielectric Properties of Nb-doped $\text{CaCu}_3\text{Ti}_4\text{O}_{12}$ Electroceramics Measured at High Frequencies (Sulaiman et al., 2010).</p>	<p>-Doped by Nb_2O_5 on Ti site of CCTO with 1 to 10 mol% of doping.</p> <p>-Wet milling process.</p> <p>-The dielectric properties of CCTO were measured at frequencies range from 1 MHz to 1 GHz.</p>

This work.	-Doped by MgO on Ca and Cu site of CCTO with 1 to 10 mol% of doping. -Wet milling process. -The dielectric properties of CCTO was measured at frequencies range from 1 MHz to 1 GHz.
------------	--

1.3 Research Objective

The objectives of this study are:

- I. To synthesize the undoped and Mg-doped $\text{CaCu}_3\text{Ti}_4\text{O}_{12}$ ($\text{Ca}_{1-x}\text{Mg}_x\text{Cu}_3\text{Ti}_4\text{O}_{12}$ and $\text{CaCu}_{3-x}\text{Mg}_x\text{Ti}_4\text{O}_{12}$) from starting materials of CaCO_2 , CuO , TiO_2 and MgO via solid state reaction method.
- II. To investigate the crystal structure and morphology of prepared CCTO samples.
- III. To investigate dielectrical properties of undoped and Mg-doped CCTO at high frequency range from 1 MHz to 1 GHz.

1.4 Research Overview

The preparation of $\text{CaCu}_3\text{Ti}_4\text{O}_{12}$ (CCTO) and Mg-doped CCTO were carried out using solid state reaction method. First step, the raw materials were characterized using X-ray Diffraction (XRD) and Scanning Electron Microscopy (SEM) to identify the phase formation and the morphology of the raw materials. The starting raw materials were CaCO_3 , CuO , and TiO_2 for undoped CCTO and MgO were added for Mg-doped CCTO. The stoichiometric of CaCO_3 , CuO , and TiO_2 were mixed together in a mole ratio of 1:3:4 for undoped CCTO. For Mg-doped CCTO, dopant source of

MgO with $x = 0.01, 0.02, 0.03, 0.05$ and 0.10 was added to form $\text{Ca}_{1-x}\text{Mg}_x\text{Cu}_3\text{Ti}_4\text{O}_{12}$ and $\text{CaCu}_{3-x}\text{Mg}_x\text{Ti}_4\text{O}_{12}$. The raw materials were wet milled using acetone, deionized water and ethanol as wetting agent and zirconia ball as the milling medium. The weight ratio between mixed powder and ball mill is 1:10. The process was done for 1 hour. The wet ball milling process is believed can produce the homogenous samples, faster than dry milling process. It is because high dispersion and high mobility of particles can assist small quantity of doping element to disperse properly (Moulson and Herbert, 2003).

The mixture powder was dried overnight in oven at temperature 100°C . The dried powder was ground using agate mortar and calcined at 900°C using Electrical Carbolite Furnace for 12 hours. The heating rate is $5^\circ\text{C}/\text{minute}$. The calcination's temperature and soaking time were chosen based on previous study by Mohamed et al. (2007). After that, the yellowish powder was ground and the phase formation of calcine powder was characterized using XRD. The powder was then pressed at 300 MPa to form pellet sample with a diameter of ~ 6 mm and ~ 12 mm and a thickness of ~ 1.2 mm by using hydraulic hand press. The green pellets were sintered in air at 1020°C , 1030°C and 1040°C using High Temperature Tube Furnace for 12 hours. The heating rate for sintering process is $5^\circ\text{C}/\text{minute}$.

The sintered samples were then subjected to XRD in order to identify the phase formation and crystal structure of the samples. Meanwhile the microstructures and elemental composition of the samples were observed using SEM and Energy Dispersive X-ray (EDX). The density of samples was determined using Archimedes principles. Finally, in order to measure the electrical behavior of the samples, a flat uniform surface of pellet was prepared by polishing the samples using grinding machine. After cleaned using ultrasonic machine, the surfaces were coated by silver

paste which acts as electrodes. The dielectric properties of pellet samples were measured using Impedance Analyzer at frequency range of 1MHz to 1GHz. The flow chart for the experimental work was illustrated in Figure 1.1.

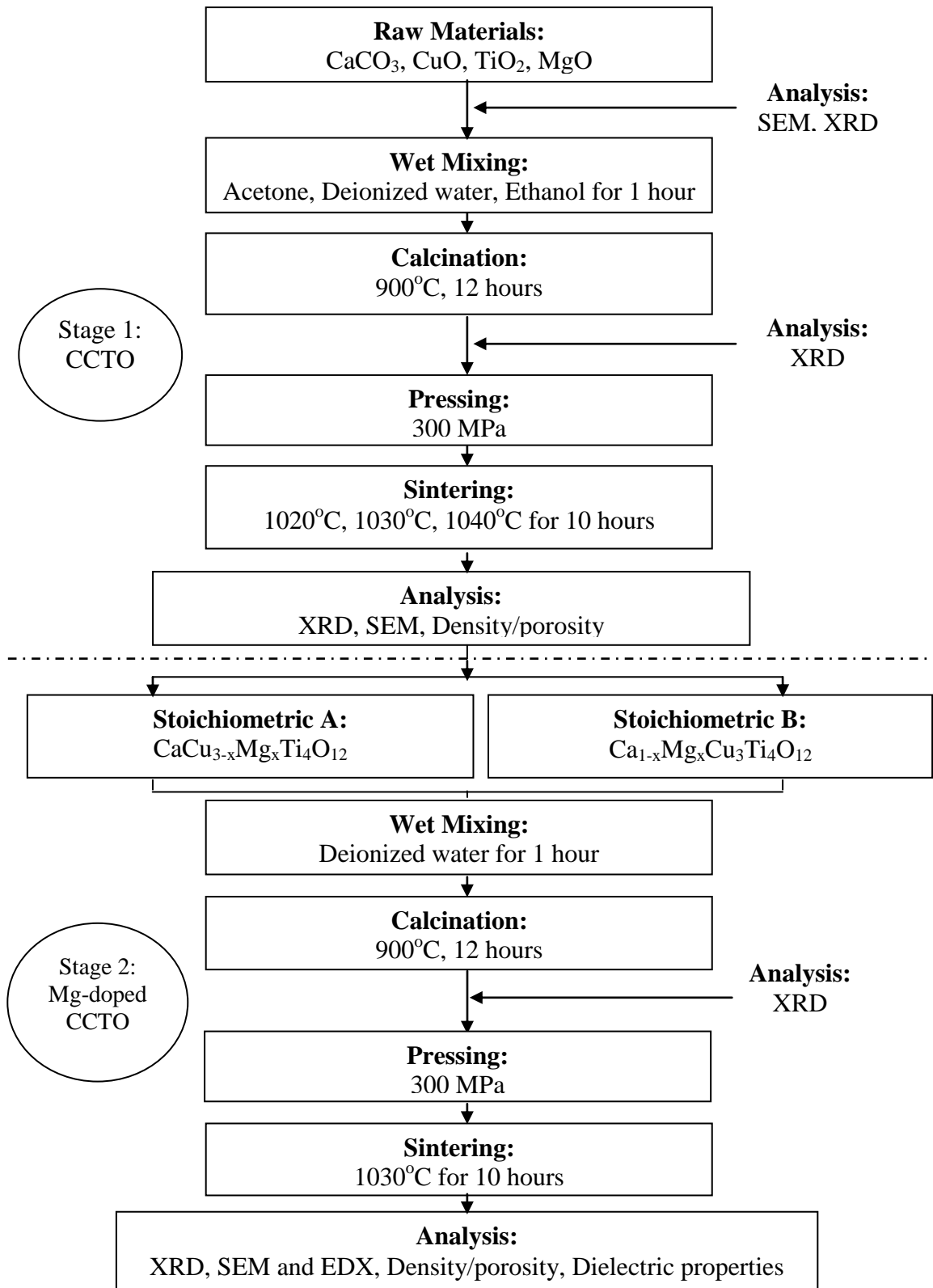


Figure 1.1: Process flow of undoped and Mg-doped CCTO with $x = 0.00, 0.01, 0.02, 0.03, 0.05, 0.10$.

CHAPTER 2

LITERATURE REVIEW

2.1 Introduction

The term electroceramic is used to explain a class of ceramic materials that have been formulated or being used specially for electrical, magnetic or optical properties. The unique properties of electroceramic make it important nowadays particularly in many key technologies including electronics, energy conversion and storage and also for communications. Their properties can be modified in order to fabricate a product that can be used as insulators, electrodes, sensors and capacitors. There are seven types of electroceramic materials which are ceramic insulators, dielectric ceramics, piezoelectric ceramics, ferroelectric ceramics, magnetic ceramics, superconductors and photonic ceramics.

Ceramic that used for microwave device application need a good dielectric properties which is high dielectric constant (>1) and low dielectric loss (<0.001) (Belous and Ovchar, 2010). High dielectric constant has been found in oxide types of $ACu_3Ti_4O_{12}$ (A= trivalent rare earth or Bi). The $ACu_3Ti_4O_{12}$ compound family has been discovered since 1967 but the dielectric properties of this perovskite structure was not examined. Ramirez et al. (2000) have reported that CCTO can possess colossal dielectric constant at room temperature and nearly temperature independent at range 100 - 400K. Due to large dielectric value, CCTO turned out to be an attractive material for high energy density capacitor. Thus, it can be use to enhance performance and reduce the dimensional size of microelectronic devices.

2.2 Dielectric Materials

Dielectric materials are electrical insulators but can be polarized in the presence of an electric field and also containing an electrostatic field within them under the state of polarization (Callister, 2007). When dielectric materials were placed in the electric field, electric charges do not flow or conduct through the material. However, the charges were slightly shifting from their average equilibrium positions which cause dielectric polarization. Due to dielectric polarization, there is separation between positive and negative charges. Positive charges shift toward the field while negative charges move to the opposite direction. Then, the internal field will be created (Britannica, 2009).

Dielectric is usually used to explain the materials with high polarizability which is expressed by the value of dielectric constant and also to show the energy storing capacity of the material (Callister, 2007). The electrostatic field can store energy if current flow between electric charge poles can be kept to a minimum and electrostatic flux is not interrupted and not impeded. This property is very important for the electronic device application such as capacitors, particularly at radio frequencies (Rouse, 2010).

Most of dielectric materials are in solid form but some of liquids and gases can also be classified as dielectric materials. The examples of dielectric materials are porcelain, glass, distilled water and dry air. A vacuum condition is also a very efficient dielectric (Rouse, 2010).

2.3 Dielectric Properties

The main property of dielectric is being able to support the electrostatic field while dissipating minimal energy in the form of heat. The most common dielectric

properties are dielectric constant and dielectric loss. The dielectric constant or relative permittivity is a ratio of permittivity of dielectric medium over permittivity of a vacuum (Sharif, 2010). It also indicates the change in charge stored in the capacitor. The total charge stored in the capacitor will change when a dielectric material is introduced between two opposite plates of capacitor. But, the change of charge stored is depending on the capability of the dielectric materials to polarize under the electric field (Sharifuddin, 2007).

Material with high dielectric constant is needed for the application of capacitor. Generally, the materials such as metal oxides have high dielectric constant. Materials with moderate dielectric constant consist of ceramic, glass, paper, mica, polyethylene and distilled water. Meanwhile, vacuum, dry air and dry gases (helium and nitrogen) are the examples of low dielectric constant substances (Rouse, 2010). An ideal dielectric material is the one that exhibit high dielectric constant and low dielectric loss. The lower dielectric loss, the dielectric material can be more effective to be used as device. It is because of less energy will dissipate as heat when low dielectric loss material operated as a device. High dielectric loss will raise the temperature of the dielectric material.

Dielectric loss can be referred as energy lost as a heat. It also can be called as dissipation factor or tangent loss ($\tan \delta$). Fowler (1994) stated that dielectric loss is happened because of the dipoles that continually reorient with the field. A little electric energy will be dissipated or converted into the heat energy on every time the molecular structure of the dielectric material has to adjust to a new polarity. The dielectric loss is also influenced by the ion vibration and ion migration which is depending on the temperature and frequency (Gao and Sammes, 1999).

The capacitance, C is related to the quantity of charge stored, Q on positive and negatively charge plates when a voltage, V was applied across the capacitor with the electric field directed from positive to the negative plates. The capacitance is calculated using Equation (2.1).

$$C = \frac{Q}{V} \quad (2.1)$$

Farads (F) or coulombs per volts are the unit of capacitance. If the region between the plates is filled with a vacuum like as shown in Figure 2.1 (a) the capacitance can be obtained from the Equation (2.2):

$$C = \epsilon_0 \frac{A}{l} \quad (2.2)$$

where ϵ_0 is the permittivity of a vacuum, which is a constant that have the value of 8.85×10^{-12} F/m . The area of plates is representing by A and l is the length distance between the plates. Meanwhile, the capacitance of the capacitor can be calculated using Equation (2.3) if the dielectric materials are place into the area within the plates as shown in Figure 2.1 (b)

$$C = \epsilon \frac{A}{l} \quad (2.3)$$

where ϵ stand for permittivity of the dielectric material, which is greater values than ϵ_0 . Then, the dielectric constant or the relative permittivity ϵ_r can be obtained from Equation (2.4) by using this ratio;

$$\epsilon_r = \frac{\epsilon}{\epsilon_0} \quad (2.4)$$

Based on this equation, this represents the increasing value of charge storing capacity when dielectric medium is place compared when vacuum region was in between the plates (Callister, 2007).

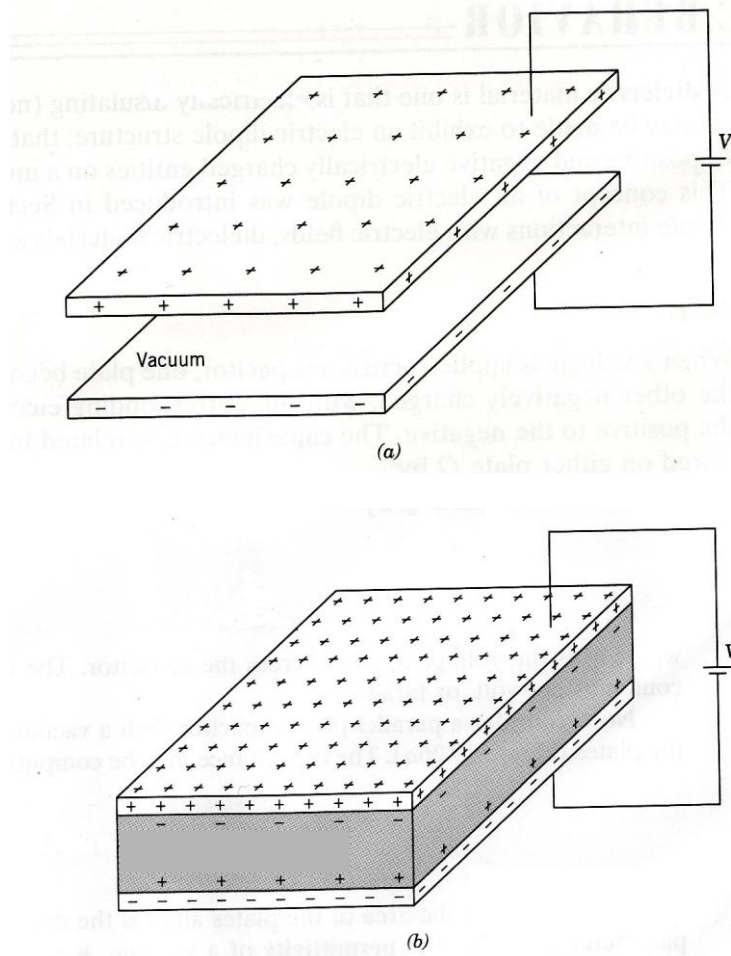


Figure 2.1: A parallel-plate capacitor (a) in a vacuum and (b) when a dielectric material is present (Callister, 2007).

Referring to the Figure 2.1, the relative permittivity ϵ_r increase after the dielectric material is inserted. The examples of dielectric constant value of some dielectric materials were listed in Table 2.1.

Table 2.1: The value of dielectric constant of materials measured at 1 MHz (Young and Frederikse, 1973).

Material	Dielectric Constant	Dielectric Loss
Alumina	8.5	4
Porcelain	5.5	3.75
Rutile	80	0.375
Calcium titanate	150	3
Lead zirconate	110	30
Magnesium titanate	14	0.25
Strontium titanate	200	5

2.4 Polarization Effect

The basic model of polarization within the dielectric material was being used to explain the increase in capacitance or dielectric constant. Polarization is the arrangement of induced atomic or molecular dipole moments with the help of external applied field. There are three kinds of polarization which are electronic polarization, ionic polarization and orientation polarization. Usually, dielectric materials show at least one of these types which is also depend on the material and the manner of externally applied field (Callister, 2007).

Electronic polarization occurs when the center of negative charged electron cloud was shift in relation to the positive atom nucleus by the electric field (Figure 2.2 (a)). This phenomenon exists when electric field is present and can be found in all dielectric materials. Meanwhile, ionic polarization is happened when applied field tends to shift cations and anions in opposite direction which will increase a net dipole moment. As shown in Figure 2.2 (b), this phenomenon occurs only in ionic materials.

Figure 2.2 (c) shows the orientation polarization. Orientation polarization is related with the existence of permanent electric dipoles which present even in the absence of an electric field (Callister, 2007).

The sum of these three types of polarization is equal to the total polarization P of a material which is shown in Equation (2.5).

$$P = P_e + P_i + P_o \quad (2.5)$$

Where;

P_e = electronic polarization,

P_i = ionic polarization

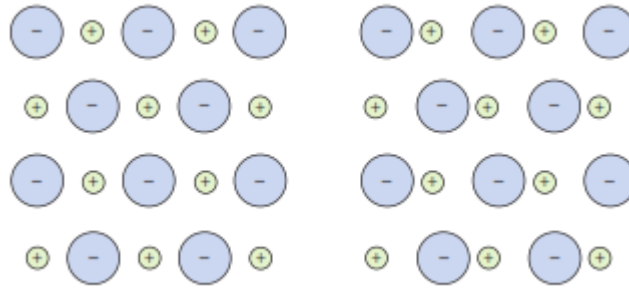
P_o = orientation polarization.

But, probably one or more of these polarizations to be absent for total magnitude polarization is also possible (Callister, 2007).

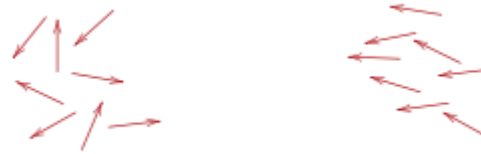


(a)

Figure 2.2: Schematic representation of different mechanism of polarization (a) Electronic polarization (b) Ionic polarization (c) Orientation polarization (Callister, 2007) (cont.).



(b)



(c)

Figure 2.2: Schematic representation of different mechanism of polarization (a) Electronic polarization (b) Ionic polarization (c) Orientation polarization (Callister, 2007).

2.4.1 Frequency Dependence on the Dielectric Constant

If a dielectric material is subjected to the polarization by an ac electric field, the dipoles attempt to reorient with the field for each reversal and it requires some finite time. Some minimum reorientation time exists for each polarization type and relaxation frequency is taken as the reciprocal of this minimum reorientation time. Relaxation frequency is the reciprocal of the minimum reorientation time for an electric dipole within the alternating electric field (Callister, 2007) and it is determined when there are abrupt drop of the dielectric constant (Tripathi et al., 2009).

A dipole cannot keep shifting orientation direction when the frequency of the applied electric field exceeds its relaxation frequency. So, it will not make a

contribution to the dielectric constant. As shown in Figure 2.3, the dependence dielectric constant, ϵ_r on the field frequency exhibits all three types of polarization. When a polarization mechanism ceases to function, there is an abrupt drop in the dielectric constant. Otherwise, dielectric constant is virtually frequency independent (Callister, 2007).

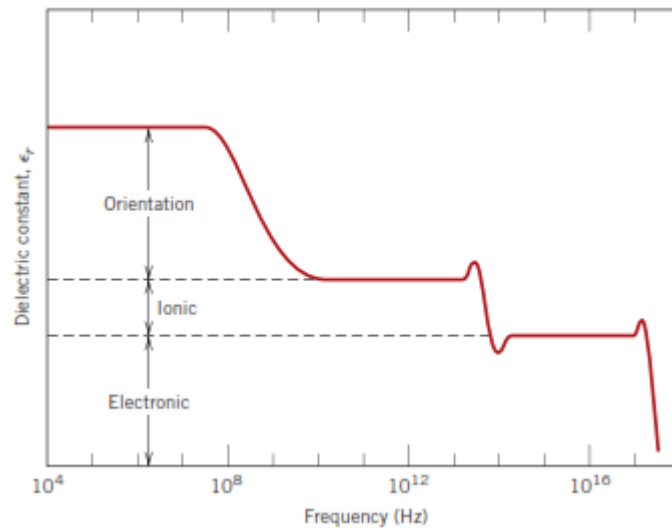


Figure 2.3: Variation of dielectric constant with the frequency of an alternating dielectric field (Callister, 2007).

2.5 Perovskite Structure

Perovskite mineral was first discovered in 1839 by Gustav Rose, a mineralogist from Russia (Lemanov et al., 1999). Perovskite is a group of calcium titanium oxide mineral or calcium titanate, with the molecular formula CaTiO_3 . ABO_3 is a general chemical formula for perovskite structure, where A and B are two different sizes of cations and O is an anion that bond to both cations. Usually, the cation A is larger than cation B.

Cubic unit cell is the most symmetry perovskite structure. Cation A is locates at the corner position, cation B is places at body centre position and anion O is sits at

face centre position (Jonker & Santen, 1950). This arrangement can be visualized as perovskite related body centered cubic (bcc). The ideal cubic symmetry of perovskite structure is it has the cation A in 12-fold cuboctahedral coordination and cation B in 6-fold coordination which was surrounded by an octahedron of anion (Gorrín, 2012). The diagram of perovskite structure of ABO_3 is shown in Figure 2.4.

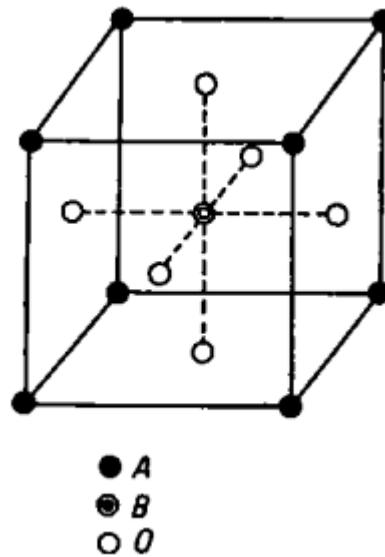


Figure 2.4: Unit cell of perovskite cubic structures (Jonker & Santen, 1950).

Due to the relative ion size conditions for stability of the cubic structure are quite tight, any small distortion and buckling can create several lower-symmetry distorted versions. Low-symmetry distortion might come from small distortion of the crystal structure which causes the structure to be elongated or compressed like cubic to orthorhombic (Raveau and Seikh, 2012). So, it will reduce the coordination number of cations A, cations B or both of the cations. For example, tilting of the BO_6 octahedra can lessen the coordination number of cations A. The resulting electric dipole after the presence of electric field is responsible for the property of

ferroelectricity and it was shown by perovskites material such as BaTiO_3 that distort in this way.

Any material that has same chemical formula of ABO_3 can be known to have perovskite structure. The examples of materials that have perovskite structure are MgTiO_3 , BaTiO_3 , CaTiO_3 , and $\text{CaCu}_3\text{Ti}_4\text{O}_{12}$. Perovskite structure can possess high values of dielectric and this class of materials was widely used in technological applications such as capacitors, ferroelectrics, superconductors, and sensors (Sanchez- Benitez et al., 2004).

2.6 $\text{CaCu}_3\text{Ti}_4\text{O}_{12}$

$\text{CaCu}_3\text{Ti}_4\text{O}_{12}$ (CCTO) is a family member of $\text{ACu}_3\text{Ti}_4\text{O}_{12}$ that was first discovered by Deschanvres et al. (1967). CCTO is one of the compounds that have perovskite structure besides MgTiO_3 , BaTiO_3 and CaTiO_3 . Based on general formula of perovskite structure (ABO_3), He et al. (2002) stated that CCTO has perovskite related body centered cubic which Ca^{2+} and Cu^{2+} cations located in the A-sites while Ti^{4+} cations is placed at B-site. As shown in Figure 2.5, the Ti^{4+} ions are surrounded by 6 oxygen ions, forming TiO_6 octahedra. The size mismatch between Ca^{2+} and Cu^{2+} ions causes TiO_6 octahedra to undergo substantial tilting. Manik and Pradhan (2006) mentioned that the tilt angle of TiO_6 octahedra is nominally at 141°

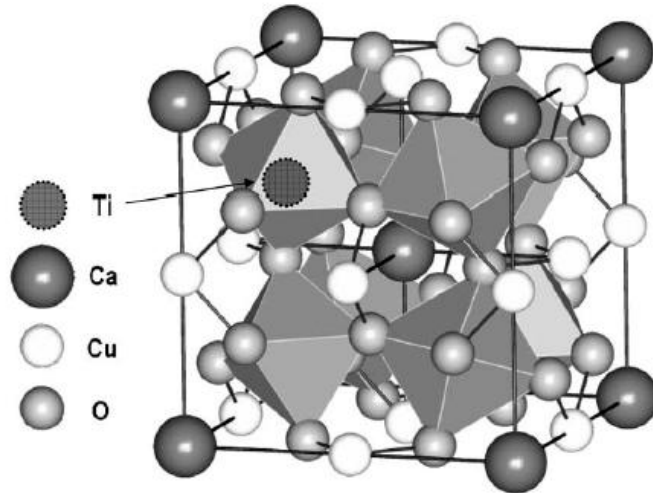


Figure 2.5: Unit cell of body-centered cubic $\text{CaCu}_3\text{Ti}_4\text{O}_{12}$ in the $\text{Im}\bar{3}$ space group (Manik and Pradhan, 2006).

CCTO has been attracted a great attention by researchers due to its unusual dielectric property. Among 13 members of $\text{ACu}_3\text{Ti}_4\text{O}_{12}$ family, CCTO show the most exceptional behavior. It exhibits large dielectric constant ($\sim 10^4$) at room temperature and almost constantly keeps it at low frequencies over the wide temperatures range from 100 to 400 K. However, when the temperature is below ~ 100 K, the dielectric constant drops rapidly to a value ~ 100 without any detectable changes by any structural phase transition after probed by neutron powder diffraction (Ramirez et al., 2000). The dramatic decrease might be due to the dipoles “freeze” or relax out at low temperatures (Sinclair et al., 2002). The dielectric properties of 13 members of $\text{ACu}_3\text{Ti}_4\text{O}_{12}$ family that were measured at frequency 100 kHz are shown in Table 2.2. From Table 2.2, it found that CCTO possesses high dielectric constant and low dielectric loss compared to the others $\text{ACu}_3\text{Ti}_4\text{O}_{12}$ family.

Table 2.2: Dielectric properties data and lattice parameter data for $\text{ACu}_3\text{Ti}_4\text{O}_{12}$ phases at 25°C (Subramanian et al., 2000).

Compound	Relative dielectric constant	Loss tangent	Lattice parameter
$\text{CaCu}_3\text{Ti}_4\text{O}_{12}$	10,286	0.067	7.391
$\text{CdCu}_3\text{Ti}_4\text{O}_{12}$	409	0.093	7.384
$\text{La}_{2/3}\text{Cu}_3\text{Ti}_4\text{O}_{12}$	418	0.060	7.427
$\text{Sm}_{2/3}\text{Cu}_3\text{Ti}_4\text{O}_{12}$	1,665	0.048	7.400
$\text{Dy}_{2/3}\text{Cu}_3\text{Ti}_4\text{O}_{12}$	1,633	0.040	7.386
$\text{Y}_{2/3}\text{Cu}_3\text{Ti}_4\text{O}_{12}$	1,743	0.049	7.383
$\text{Bi}_{2/3}\text{Cu}_3\text{Ti}_4\text{O}_{12}$	1,671	0.065	7.413
$\text{BiCu}_3\text{Ti}_3\text{FeO}_{12}$	692	0.082	7.445
$\text{LaCu}_3\text{Ti}_3\text{FeO}_{12}$	44	0.339	7.454
$\text{NdCu}_3\text{Ti}_3\text{FeO}_{12}$	52	0.325	7.426
$\text{SmCu}_3\text{Ti}_3\text{FeO}_{12}$	52	0.256	7.416
$\text{GdCu}_3\text{Ti}_3\text{FeO}_{12}$	94	0.327	7.409
$\text{YCu}_3\text{Ti}_3\text{FeO}_{12}$	33	0.308	7.394

Realized of its special properties has led the researchers to discuss the possible origin of this abnormally high dielectric constant in terms of its crystal structure. Several models have been suggested to explain the dielectric behavior of CCTO which are classified into two causes; intrinsic mechanism and extrinsic mechanism. Intrinsic mechanism defines that huge dielectric constant of CCTO is measured in single domain crystal, defect free and perfectly stoichiometric while

extrinsic mechanism term is means that the dielectric response is related with domain boundaries, defects or other crystalline deficiencies (He et al., 2002).

Subramanian et al. (2000) had suggested that the high dielectric constant of CCTO may arise from the local dipole moments. It was related with off-center displacement of Ti^{4+} ions due to the site symmetry for Ti^{4+} ions in CCTO is lower than in cubic BaTiO_3 . But, the transition to a ferroelectric state like BaTiO_3 is being obstructed by the tilt TiO_6 octahedra due to the TiO_6 octahedra was required to accommodate the square planar coordination of Cu^{2+} ions.

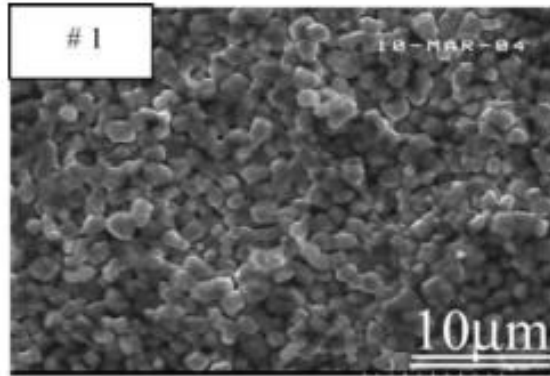
However, Sinclair et al. (2002) reported that the giant dielectric phenomenon is attributed to an internal barrier layer capacitance (IBLC) instead of an intrinsic property of the crystal structure. After carried out by using impedance microscopy measurement, it demonstrated that CCTO is electrically heterogeneous which consist of semiconducting grains and insulating grain boundaries. So, the presence of thin insulating layer at grain boundaries prevents the entire sample to be conductive.

2.7 Grain Size Effect

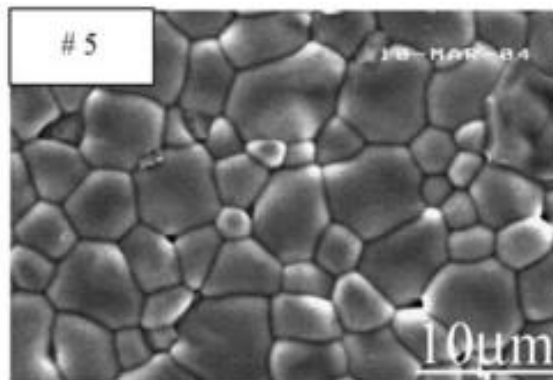
One of the factors that contributed to the unique dielectric properties of CCTO can be related to the microstructural grains. Most of the researchers claim that giant dielectric constant is interrelated with larger grain size. Therefore, many researchers studied the relationship between the microstructural grains and dielectricity of CCTO.

Brizè et al. (2006) reported that the huge dielectric constant can be correlated with the grain size effect. The dielectric constant for the sample with grain size around $\sim 1.3 \mu\text{m}$ (sample no. 1 in Figure 2.6 (a)) was lower than the sample with large grain size ($\sim 4.1 \mu\text{m}$) (sample no. 5 in Figure 2.6 (b)). As illustrated in Figure 2.7, at

frequency 10 Hz, the dielectric constant of the sample no. 5 was about ~9000 while it reached only ~3000 for the sample no. 1 that has smaller grain size compared to the sample no. 5.



(a)



(b)

Figure 2.6: SEM images of CCTO surface of sintered pellets No. 1 and No. 5 at 1000°C for 20 hours (# is referring to the number of samples) (Brizè et al. (2006)).